Shear response of a frictional interface to a normal load modulation

L. Bureau, T. Baumberger, and C. Caroli
Groupe de Physique des Solides, 2 place Jussieu, 75251 Paris Cedex 05, France*
(Received 30 May 2000)

We study the shear response of a sliding multicontact interface submitted to a harmonically modulated normal load, without loss of contact. We measure, at low velocities ($V<100\ \mu m\,s^{-1}$), the average value $\overline{F}$ of the friction force and the amplitude of its first and second harmonic components. The excitation frequency ($f=120$ Hz) is chosen much larger than the natural one, associated with the dynamical aging of the interface. We show the following: (i) In agreement with the engineering thumb rule, even a modest modulation induces a substantial decrease of $\overline{F}$. (ii) The Rice-Ruina state and rate model, though appropriate to describe the slow frictional dynamics, must be extended when dealing with our ''high'' frequency regime. That is, the rheology which controls the shear strength must explicitly account not only for the plastic response of the adhesive junctions between load-bearing asperities, but also for the elastic contribution of the asperities bodies. This ''elastoplastic'' friction model leads to predictions in excellent quantitative agreement with all our experimental data.

PACS number(s): 46.55.+d, 68.35.Ja, 83.50.Nj

I. INTRODUCTION

Friction between solids carrying a time-dependent normal load is a subject of interest in different fields, from mechanical engineering, where the ''friction-lowering'' effect of external vibrations is well known [1] and commonly used in applications, to geophysical studies of the effect of rapid stress changes on static and dynamic friction of rocks [2,3], aiming at a better understanding of the coupling between normal and tangential stress states on slipping faults [4–6].

These studies involve multicontact interfaces (MCI's), i.e., interfaces between macroscopic solids with rough surfaces. The real area of contact thus consists of a large number of small contacts with sizes on the micrometer scale.

In a situation of constant normal load on the MCI, the phenomenological state- and rate-dependent friction (SRF) model, formulated by Rice and Ruina [7], successfully describes the details of the low-velocity dynamics (typically in the 0.01–100 $\mu m\,s^{-1}$ range) of such systems, such as the bifurcation between steady state and stick-slip oscillations [8]. The model states that the dynamic friction force F_{fr} depends on the instantaneous sliding velocity $\dot{x}$ and on a dynamic state variable Φ as

$$F_{fr}(\dot{x},\Phi)=W\left[\mu_0+A\ln\left(\frac{\dot{x}}{V_0}\right)+B\ln\left(\frac{V_0\Phi}{D_0}\right)\right], \qquad (1)$$

where μ_0 is the dynamic friction coefficient in steady sliding at the reference velocity V_0, and A and B are measured to be positive and of typical order 10^{-2} (with $B>A$).

The state variable Φ can be interpreted as the ''age'' of the MCI, i.e., the average duration of the transient contact between load bearing asperities. For example, in stationary sliding at velocity V, the set of microcontacts is destroyed and replaced by a new one over a characteristic sliding length D_0, and the state variable is thus expressed as $\Phi=D_0/V$.

More generally, the model specifies the time evolution law of Φ as

$$\dot{\Phi}=1-\frac{\dot{x}\Phi}{D_0}. \qquad (2)$$

In Eq. (1), the two corrections to μ_0 have distinct physical meanings: the first term describes an instantaneous velocity strengthening of the interface, while the second expresses strengthening of the interface with its ''age,'' which in stationary sliding, where $\Phi=D_0/V$, leads to a velocity-weakening effect.

In the spirit of the Bowden and Tabor analysis [9], for a MCI, one can write the friction force as [10]

$$F_{fr}=\sigma_s(\dot{x})\Sigma_r(\Phi,W), \qquad (3)$$

where σ_s defines an interfacial shear strength, Σ_r is the real area of contact between the solids, and W is the normal load carried by the multicontact interface. The age-strengthening effect is associated with the creep growth of the microcontact area under normal load:

$$\Sigma_r(\Phi,W)=\Sigma_0(W)\left[1+\xi\ln\left(\frac{\Phi V_0}{D_0}\right)\right]. \qquad (4)$$

Σ_0—the real area of contact at $\Phi=D_0/V_0$—exhibits a linear dependence on W, as explained by Greenwood and Williamson's model [11] of contact between rough surfaces. That is, the friction force obeys the Amontons law $F_{fr}\propto W$.

The velocity-dependent interfacial strength of the interface is described as:

$$\sigma_s(\dot{x})=\sigma_{s0}\left[1+\eta\ln\left(\frac{\dot{x}}{V_0}\right)\right], \qquad (5)$$

*Associé au Centre National de la Recherche Scientifique et aux Universités Paris 6 et Paris 7.

This form for the interface ''rheology,'' discussed in detail in Ref. [10], results from the thermally activated depinning of multistable nanometric units localized in a layer of nanometric thickness forming a junction between micrometric asperities. Equations (4) and (5) yield Eq. (1) with $\mu_0 = \sigma_{s0}\Sigma_0/W$, $\xi = B/\mu_0$, and $\eta = A/\mu_0$. Also, since $\xi, \eta \ll 1$, non-linear logarithmic terms can be neglected.

The SRF model, and its physical interpretation presented above, have been validated by friction experiments on different classes of contacting materials, namely, granite, paper, polymer glasses, and elastomers, under constant normal load applied to the solids.

In the case of a time-dependent normal load, one can first note that in the Amontons-Coulomb description ($F_{fr} = \mu W$, with constant μ), a change in W would lead to a proportional change in F_{fr}, in particular a harmonic normal load modulation $W = W_0(1 + \epsilon \cos(\omega t))$ would produce a harmonic frictional modulation about a nonmodified average value μW_0.

In the SRF framework, the variations of $\dot{x}$ and Φ are nonlinearly coupled, through Eqs. (1) and (2), to the load modulation, thus resulting in nontrivial effects on the friction force (such as, for instance, an anharmonic response to a harmonic normal load). However, the model as expressed by Eqs. (1) and (2) may not be sufficient to describe correctly the frictional response for the following reasons: (i) the interface rheology expressed by Eq. (5) may not hold for ''fast'' changes of W; and (ii) the load variation may modify the interface age strengthening process, thus leading to changes in the evolution of Σ_r with Φ, or in the evolution law of the state variable Φ itself.

Based on their results on the response to normal stress steps and pulses in granite friction experiments, Linker and Dieterich [2] suggested modifying the evolution law of Φ, while retaining the functional form [Eq. (4)] of the Φ dependence of Σ_r. Arguing that a sudden change in normal stress would result in a sudden change in Φ, they postulated

$$\dot{\Phi} = 1 - \frac{\dot{x}\Phi}{D_0} - \frac{\alpha\dot{\sigma}}{B\sigma}\Phi, \tag{6}$$

where they inferred $\alpha = 0.2$, for granite, from their analysis of the response to sudden normal load steps.

In a recent study, Richardson and Marone [3] investigated the influence of normal stress modulations on the so-called ''frictional healing'' effect in a granular material layer confined between rough granite blocks: starting from steady sliding, shear loading is stopped, and the subsequent shear stress relaxation is measured in presence of a 1-Hz normal load modulation (a modulation frequency close to the characteristic stick-slip oscillations frequency that can be inferred for their system).

Friction experiments with confined granular media have been successfully described by the SRF model in situations of constant normal load [12] (although the physical meaning of the variable Φ is not clear yet for these systems). However, the use of the constitutive law proposed by Linker and Dieterich to include the time dependence of the normal load did not account properly for the details of the results obtained by Richardson and Marone, in particular the amplitude of stress relaxation after stopping the drive, and the height of the stress overshoot after resuming loading.

In this paper we present an extensive study of the effect of a harmonic modulation of the normal load, $W = W_0(1 + \epsilon \cos(\omega t))$, on the dynamic frictional response of a multicontact interface. Experiments are conducted on an interface between two blocks of poly(methyl-metacrylate) (PMMA), at velocities $V < 100\ \mu\mathrm{m\,s^{-1}}$, a load modulation frequency $f = 120\ \mathrm{Hz} \gg V/(2\pi D_0)$, and a relative amplitude ϵ in the range 5×10^{-3}–0.5 (so that no loss of contact between the surfaces occurs).

We study quantitatively the average $\overline{F}$ and the components at frequency f and $2f$, F_1 and F_2, of the tangential pulling force,

$$F = K(Vt - x) = M\ddot{x} + F_{fr} \tag{7}$$

for different values of V and ϵ; these results are presented in Sec. II. We find in particular that the modulation of W induces a systematic decrease of the average dynamic friction coefficient $\overline{\mu} = \overline{F}/W_0$. This effect, which increases with higher ϵ, is quite substantial: a typical magnitude of this effect is a 20% decrease of $\overline{\mu}$ for $\epsilon = 0.5$.

To analyze our experimental data quantitatively, we need to evaluate which fraction, ϵ_{eff}/ϵ, of the load modulation is effectively borne by the microcontacts. Indeed, the normal load modulation is too fast for air to be drained in and out of the micrometer-thick interfacial gap. We have studied this ''leaking air cushion'' effect by conducting similar experiments under a primary vacuum. From these experiments we infer that $\epsilon_{eff}/\epsilon \approx 0.4$, and we use this in the subsequent analysis as a scaling factor for the modulation amplitude. Section III is devoted to the analysis of these results in terms of the SRF model and its possible extensions to fast load modulations:

(i) We first test the unmodified SRF model by setting in Eq. (1) $W \rightarrow W(t)$ and using the evolution law [Eq. (2)] for the state variable Φ. Numerical integration of these equations leads to a quantitatively good prediction of the average friction force $\overline{F}(\epsilon)$. However, the predicted oscillating tangential force components F_1 and F_2 strongly depart from the observed dependences on ϵ and V.

(ii) We then test the proposition of Linker and Dieterich. Using their evolution law [Eq. (6)] and their proposed value of $\alpha = 0.2$, we find that (i) the decrease of $\overline{F}(\epsilon)$ is much smaller than the measured values, and (ii) the agreement for F_1 and F_2 is not better than in the previous $\alpha = 0$ test.

An attempt to describe the ϵ dependence of $\overline{F}$ correctly, with a value of α small enough ($\alpha = 0.02$), leads to results close to those obtained with the basic SRF equations; this also holds for F_1 and F_2. That is, to say, as confirmed by a perturbation calculation in ϵ, our experiments do not discriminate with respect to the Linker-Dieterich evolution law for such small values of α.

Thus, this modified aging law, even if valid, does not suffice to account properly for the details of the frictional response.

(iii) We propose to modify expression (5) for the following physical reason: we know from static measurements [13] that a MCI exhibits, at shear forces much smaller than the static threshold, an elastic tangential response. One can deduce from this a shear stiffness κ_{asp} with the particular fea-

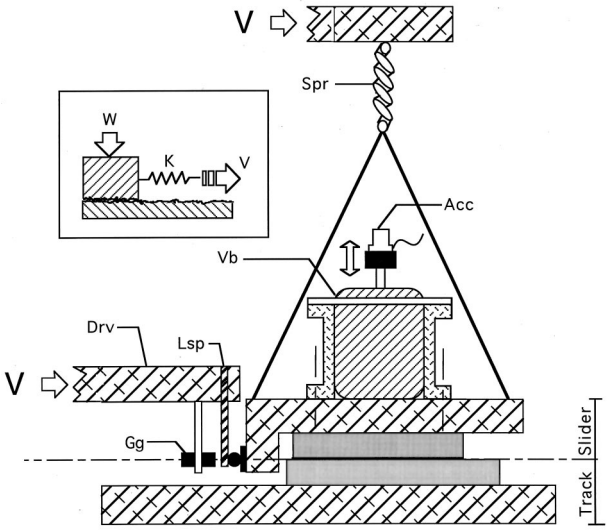

FIG. 1. Main elements of the experimental setup: translation stage (Drv); loading leaf spring (Lsp); displacement gauge (Gg); vibration exciter (Vb); weighting spring (Spr); accelerometer (Acc). The inset is the schematic representation of the spring-slider-track dynamical system with control parameters W (normal load), V (driving velocity), and K (external spring stiffness).

ture $\kappa_{asp} \propto W$. Now, in our interpretation of friction, the rate variable appearing in σ_s must be the true rate of irreversible (plastic) strain of the interfacial junction of nanometer thickness h. When taking into account the asperity elasticity κ_{asp}, strictly speaking, this strain rate reads $h^{-1}d(x-F/\kappa_{asp})/dt$. In quasistationary motion, this reduces to the $\dot{x}/h$ strain rate, hence the usual $\sigma_s(\dot{x})$ expression. In the present experimental situation, κ_{asp} is modulated as W itself, and the difference between the total and plastic strain rates becomes relevant. Indeed, we show that this extended phenomenological elastoplastic generalization of interfacial dissipation leads to a very satisfactory description of the average and oscillating shear responses to fast normal load modulations.

II. EXPERIMENTS AND RESULTS

A. Experimental setup and methods

The tribometer is composed of a slider of mass M driven along a track through a loading spring of stiffness K, one end of which is pulled at constant velocity V, as schematized in the inset of Fig. 1. The slider and track are made of PMMA [14] with nominally flat surfaces lapped with SiC powder to a roughness of order 1 μm, thus forming a multicontact interface.

A detailed drawing of the setup is given in Fig. 1. We impose the velocity V of the loading point, in the range 0.1–100 $\mu\mathrm{m\,s}^{-1}$, by means of a translation stage driven by a stepping motor. The tangential load is applied on the slider through a leaf spring of stiffness $K=0.2$ N $\mu\mathrm{m}^{-1}$, which is the more compliant part of the system. The dead weight of the slider is 16 N. The average normal load W_0 can be set in the range 3–16 N with the help of a vertical spring attached to a remote point itself translated horizontally at the pulling velocity V through a second translation stage, in order to prevent any tangential coupling.

The normal load modulation is achieved by means of a vibration exciter rigidly attached to the slider: a harmonic voltage input of given amplitude and frequency f results in a harmonic vertical motion of the moving element of the exciter on which an accelerometer is fixed. An acceleration of amplitude γ of this moving element of mass m induces a normal load modulation on the slider of amplitude $m\gamma$ at frequency f. We thus obtain a normal load $W=W_0(1+\epsilon\cos(\omega t))$ with $\omega=2\pi f$ and $\epsilon=m\gamma/W_0$ in the range 5×10^{-3}–0.5.

We use the loading leaf spring as a dynamometer by measuring its deflection ΔX by means of an eddy current displacement gauge. The tangential force applied to the slider is thus $F=K\Delta X$. We measure the average value of the output voltage of the gauge, and use a lock-in amplifier to measure the amplitude of the first and second harmonics of this output signal with respect to the harmonic excitation signal. We thus characterize the shear force through its average value $\overline{F}$ and its ac components at frequencies f and $2f$, of respective amplitudes F_1 and F_2.

The experiments are conducted according to the following protocol: for a fixed set of parameter values W_0 and V leading to steady sliding when $\epsilon=0$, we measure $\overline{\mu}(0)=\overline{F}(\epsilon=0)/W_0$. The normal load modulation is then set at amplitude ϵ, while sliding, and shear force measurements yield $\overline{\mu}=\overline{F}/W_0$, $\mu_1=|F_1|/W_0$ and $\mu_2=|F_2|/W_0$. The modulation is then switched off, and $\overline{F}(\epsilon=0)$ is systematically remeasured before setting a new value of ϵ, in order to check that no drift occurred during the measurement. Moreover, we check that for $\epsilon\neq0$ the shear force signal does not exhibit low-frequency stick-slip oscillations. The experimental results reported below have been obtained with an average load $W_0=7$ N and modulation frequencies f of 120 or 200 Hz, chosen to be away from any mechanical resonance frequency of the setup.

B. Results

1. Average dynamic friction

The effect of the normal load modulation on the average tangential force response is to systematically lower the dynamic friction coefficient. The ratio $\overline{\mu}=\overline{F}/W_0$ decreases as the modulation amplitude ϵ is increased. The variation $\Delta\overline{\mu}(\epsilon)=\overline{\mu}(\epsilon)-\overline{\mu}(0)$, plotted in Fig. 2, becomes larger than the experimental noise for $\epsilon\gtrsim0.05$, and is then quasilinear with ϵ, though it does not extrapolate to 0 at $\epsilon=0$.

Figure 3 displays measurements of $\overline{\mu}(V)$ for different values of ϵ. It appears that the only effect of an increase of the load modulation amplitude is to shift down the $\overline{\mu}(V)$ curve, without changing the slope $\partial\overline{\mu}/\partial\ln(V)$. Therefore, within experimental accuracy, $\Delta\overline{\mu}(\epsilon)$ is velocity independent.

2. ac components of the force response

The oscillating force response to a load modulation at frequency f is found to be weakly anharmonic. We characterize it by the amplitudes of the first and second harmonics μ_1 and μ_2. The ratio μ_2/μ_1 typically lies in the range 0.1–0.2.

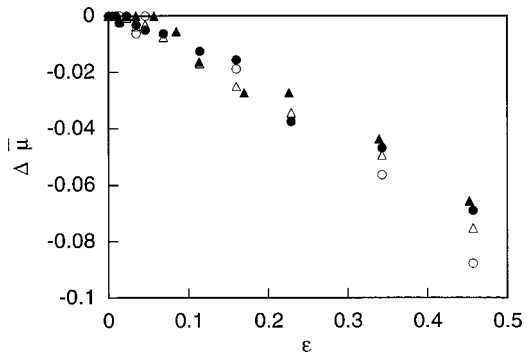

FIG. 2. Variation of the reduced average friction force $\Delta\overline{\mu} = (\overline{F}(\epsilon) - F_0)/W_0$ vs modulation amplitude ϵ at $f = 120$ Hz. Open symbols correspond to two sets of results at $V = 1\ \mu\mathrm{m\,s^{-1}}$, and full symbols to two sets at $V = 10\ \mu\mathrm{m\,s^{-1}}$.

The reduced first harmonic $\mu_1 = |F_1|/W_0$ increases monotonically with ϵ, and does not show any measurable dependence on the driving velocity, as presented in Fig. 4(a) where we plot results at $V = 1$ and $10\ \mu\mathrm{m\,s^{-1}}$. μ_1 is of order 10^{-3} at $\epsilon = 0.5$, i.e., two orders of magnitude lower than the average shift $\Delta\overline{\mu}$.

The amplitude of the second harmonic in the shear force response also exhibits a monotonic increase with the modulation amplitude. Moreover, $\mu_2(\epsilon)$ depends significantly on velocity, the measured amplitude of this component being lower for smaller V, as presented in Fig. 4(b).

3. Role of the interfacial air layer

All the above results correspond to experiments performed at atmospheric pressure. The PMMA surfaces in contact are nominally flat over typically $\Sigma_0 = 7 \times 7\ \mathrm{cm}^2$, but their roughness implies that air is trapped in an interfacial gap of micrometric thickness h_0. Any increase in normal load is borne in parallel by the microcontacts and by the interfacial air layer. This excess pressure leads the air to leak out of the edges of the sample, the rate of flow being limited by the air viscosity. For instance, when trying to lift the slider from the track, a strong suction is experienced. One may therefore expect that the air layer plays a nonnegligible role in the interfacial response to load modulation.

In order to quantify experimentally this ''leaking air cushion'' effect, we conducted a set of control experiments under

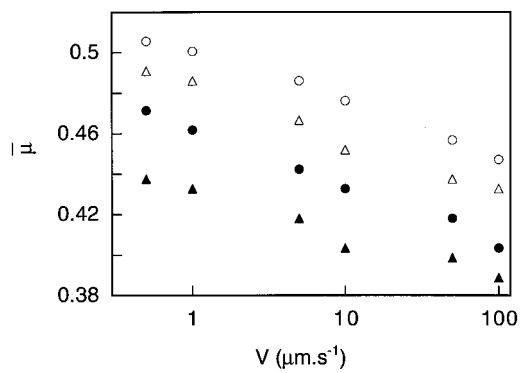

FIG. 3. Reduced average friction force $\overline{\mu}$ vs V for various values of load modulation amplitude. open circles: $\epsilon = 0$; open triangles: $\epsilon = 0.2$; full circles: $\epsilon = 0.35$; full triangles: $\epsilon = 0.5$.

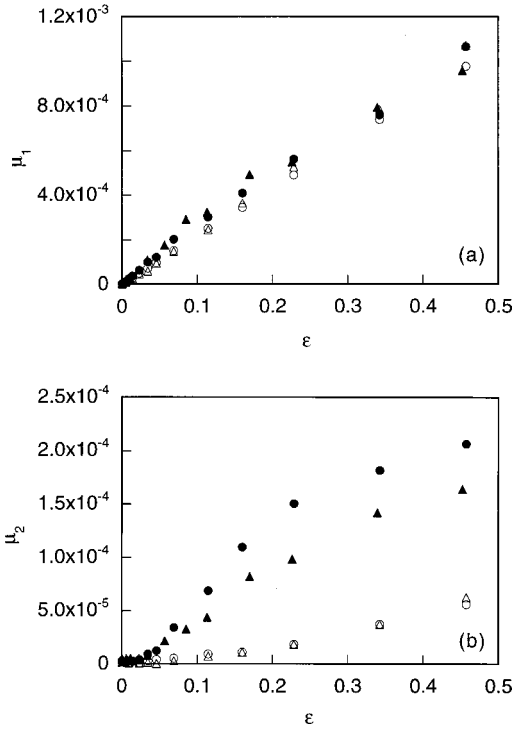

FIG. 4. Amplitude of the harmonic components of the reduced force response at $f = 120$ Hz: (a) first harmonic $\mu_1(\epsilon)$; (b) second harmonic $\mu_2(\epsilon)$. Two sets of data are plotted for each velocity: $V = 1\ \mu\mathrm{m\,s^{-1}}$ (open symbols) and $V = 10\ \mu\mathrm{m\,s^{-1}}$ (full symbols).

vacuum. The setup described in Sec. (II A) was placed in a vacuum chamber and allowed to work at pressures down to 1 mbar (a pressure at which the mean free path of air molecules becomes of order 10 μm, i.e., much larger than the interfacial gap, ensuring that the air effect has become negligible).

We first measure the average dynamic friction coefficient under constant normal load and find $\mu_0 \approx 0.5$, a value equal to the friction coefficient at atmospheric pressure. This confirms that when the interfacial air layer is simply sheared, the corresponding viscous force is negligible with respect to the solid friction one.

Then, following the protocol described in Sec. II A, we measure $\overline{\mu}(\epsilon)$, at $V = 10\ \mu\mathrm{m\,s^{-1}}$ and $f = 200$ Hz. In this control experiment we have not been able to use the frequency $f = 120$ Hz at which all other data have been obtained, due to the presence of a spurious mechanical resonance of the vacuum chamber close to 120 Hz.

A comparison of the average friction coefficient variation $\Delta\overline{\mu}$ measured at $P = 1$ atm and at $P = 1$ mbar is presented in Fig. 5. Note that for a given modulation amplitude, $|\Delta\overline{\mu}|$ is larger in vacuum than in air. Moreover, when plotted as a function of $\epsilon_{eff} = \epsilon/2.5$, the results obtained at $P = 1$ atm are found to collapse on those at $P = 1$ mbar (see Fig. 5).

In the Appendix we present a model calculation of the elastohydrodynamic response of the air layer. We show that, over the entire range of ϵ used in our experiments, the normal response of the interface is linear; hence the ratio ϵ_{eff}/ϵ does not depend on ϵ. Moreover, the estimated order of magnitude of this parameter at $f = 200$ Hz is found to be compatible with the above measured value.

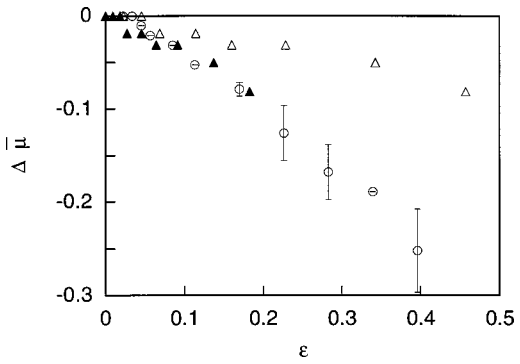

FIG. 5. Reduced average friction force $\Delta\bar{\mu}(\epsilon)$, for $V=10\ \mu\mathrm{m\,s^{-1}}$ and $f=200$ Hz at pressures $P=1$ mbar (open circles) and $P=1$ atm (open triangles). The same set of data at $P=1$ atm is also plotted (full triangles) as a function of the scaled amplitude $\epsilon/2.5$.

III. DISCUSSION AND MODEL

In this section we analyze our data within the SRF framework. The three parameters A, B and D_0 involved in the SRF laws are determined experimentally, at a constant load W, using the velocity dependence of the friction coefficient $\bar{\mu}(\ln(V))$ and the dynamic characteristics of the response close to the bifurcation threshold (this method was described in detail in Ref. [10]). For our system we measure $A=0.013\pm0.005$, $B=0.026\pm0.01$, and $D_0=0.4\pm0.04\mu$m. All the numerical integrations of SRF laws presented below are performed with this set of parameter values.

A. Rice and Ruina's model

Before coming to the question of whether or not the Rice-Ruina (RR) equations themselves should be modified in the presence of load modulations, it is reasonable to study first which response is predicted by the RR model as such. Replacing W in Eq. (1) by its instantaneous value, the equation of motion of the center of mass of the slider reads

$$M\ddot{x}=K(Vt-x)-W_0[1+\epsilon\cos(\omega t)]\left[\mu_0+A\ln\left(\frac{\dot{x}}{V_0}\right)+B\ln\left(\frac{\Phi V_0}{D_0}\right)\right], \tag{8}$$

where $x(t)$ is the instantaneous position of the center of mass of the slider with respect to the track. We assume the evolution law of Φ [Eq. (2)] to be unmodified:

$$\dot{\Phi}=1-\frac{\dot{x}\Phi}{D_0}. \tag{9}$$

1. Perturbative regime

Let us first consider the case where $\epsilon\ll1$. We linearize Eqs. (8) and (9) about the steady sliding state at velocity V, $\epsilon=0$:

$$\Phi_{st}=D_0/V,\quad x_{st}=Vt-W_0/K \tag{10}$$

Setting

$$\delta\Phi=\Phi-\Phi_{st}=\mathrm{Re}(\epsilon\Phi_1\exp(i\omega t)), \tag{11}$$

$$\delta x=x-x_{st}=\mathrm{Re}(\epsilon X_1\exp(i\omega t)), \tag{12}$$

to first order in ϵ we obtain

$$\left(-M\omega^2+K+iW_0\omega\frac{A}{V}\right)X_1+W_0\frac{BV}{D_0}\Phi_1=-W_0\bar{\mu}(V), \tag{13}$$

$$i\frac{\omega}{V}X_1+\left(i\omega+\frac{V}{D_0}\right)\Phi_1=0 \tag{14}$$

where $\bar{\mu}(V)=\mu_0-(B-A)\ln(V/V_0)$, We thus obtain

$$X_1=-\frac{W_0\bar{\mu}}{\Delta}\left(i\omega+\frac{V}{D_0}\right), \tag{15}$$

$$\Phi_1=\frac{i\omega W_0\bar{\mu}}{V\Delta}, \tag{16}$$

where Δ reads

$$\Delta=\frac{KV}{D_0}\left(\frac{\omega}{\omega_c}\right)^2\left[-\frac{K}{K_c}+\left(1-\left(\frac{\omega}{\omega_0}\right)^2\right)\left(\frac{\omega_c}{\omega}\right)^2-i\left(\frac{\omega_c}{\omega}\right)\sqrt{\frac{B-A}{A}}\left(\left(\frac{\omega}{\omega_0}\right)^2-\left(1-\frac{K}{K_c}\right)\right)\right], \tag{17}$$

and (see Ref. [10])

$$K_c=\frac{(B-A)W_0}{D_0}, \tag{18}$$

$$\omega_c=\sqrt{\frac{B-A}{A}}\frac{V}{D_0}, \tag{19}$$

respectively, are the critical stiffness and pulsation at the stick-slip bifurcation for the unmodulated system. $\omega_0=\sqrt{K/M}\approx360\ \mathrm{s^{-1}}$ is the inertial frequency.

In our experimental conditions, with $V=10\,\mu\mathrm{m\,s^{-1}}$ and $(B-A)/A\sim1$, $\omega_c\simeq25\ \mathrm{s^{-1}}$, so $\omega_c\ll\omega,\omega_0$. On the other hand $K/K_c\gtrsim1$. Then $\Delta\approx-\omega^2AW_0/V$, indicating in particular that inertia is negligible. Finally,

$$\mu_1=\frac{K|X_1|}{W_0}\epsilon=\frac{\epsilon\bar{\mu}}{A}\frac{V}{\omega}\frac{K}{W_0}. \tag{20}$$

Similarly, a second order expansion in ϵ yields the corrections at frequencies 2ω and 0, namely,

$$\mu_2\approx\frac{V}{\omega}\frac{K\bar{\mu}^2}{2W_0A^2}\epsilon^2, \tag{21}$$

$$\Delta\bar{\mu}\approx-\frac{\bar{\mu}(\bar{\mu}+2A)}{4A}\epsilon^2. \tag{22}$$

Note that Eq. (22) correctly predicts a decrease of the average friction coefficient.

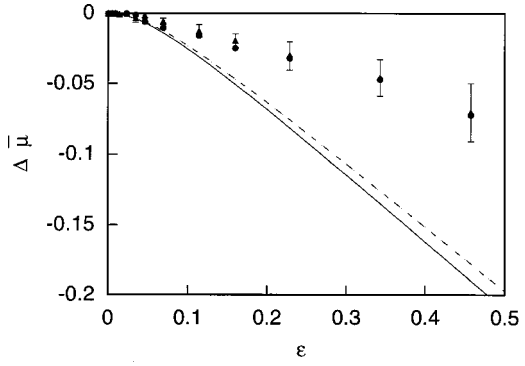

FIG. 6. Predictions of the RR model for the average friction decrease $\Delta\bar{\mu}(\epsilon)$, at $f=120$ Hz. Lines: RR model for $V=1\ \mu\mathrm{m\,s^{-1}}$ (full line), and $V=10\ \mu\mathrm{m\,s^{-1}}$ (dashed line). Symbols: raw experimental results at $V=1\ \mu\mathrm{m\,s^{-1}}$ (circles) and $V=10\ \mu\mathrm{m\,s^{-1}}$ (triangles). The experimental data have been averaged over three different runs. The error bars correspond to standard deviations on these runs.

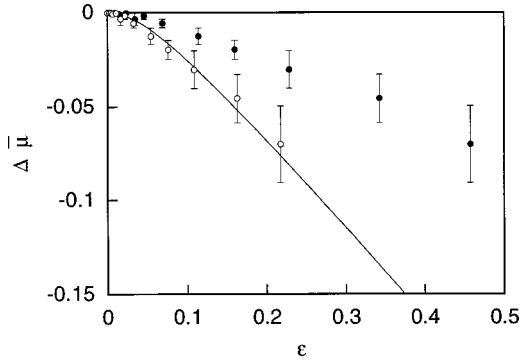

FIG. 7. Determination of ϵ_{eff} from $\Delta\bar{\mu}$. Full circles: raw experimental data at $V=1\ \mu\mathrm{m\,s^{-1}}$ and $f=120$ Hz. Open circles: the same set of data plotted as a function of $\epsilon_{eff}=\epsilon/2.1$, which provides the best agreement with the RR model prediction (line).

It is interesting to compare the relative perturbative corrections on the age and velocity variables. One finds

$$\left|\frac{\delta\Phi/\Phi_{st}}{\delta\dot{x}/V}\right|\approx\frac{\omega_c}{\omega}\ll 1, \tag{23}$$

showing that, in our regime, the modulation of the age variable contributes negligibly to the shear response.

Moreover, due to the smallness of A, the effective perturbation parameter is given by

$$\left|\frac{\delta\dot{x}}{V}\right|=\frac{\epsilon\bar{\mu}}{A}\sim 50\epsilon; \tag{24}$$

that is, the perturbative regime ($\epsilon\ll 10^{-2}$) is in practice out of experimental reach. We thus must resort to full integration of the above RR equations.

2. Average friction coefficient decrease

Numerical results for $\Delta\bar{\mu}(\epsilon)$ are plotted in Fig. 6 at excitation frequency $f=120$ Hz and velocities $V=1$ and $10\ \mu\mathrm{m\,s^{-1}}$. Note that a very weak dependence on V is predicted, as observed experimentally.

In Sec. II B we emphasized the role played by the interfacial air layer in our experiments, and pointed out that it should be taken into account through an effective modulation amplitude ϵ_{eff}, accounting for the fact that only a part of the excitation is borne by the contacting asperities. Therefore, the modulation parameter ϵ introduced in Eq. (8) must be understood as ϵ_{eff}.

On the other hand, we have measured, at $f=200$ Hz, $\epsilon_{eff}=0.4\epsilon$. As explained in the Appendix, we expect ϵ_{eff}/ϵ to exhibit some relatively weak frequency dependence. This effect depends crucially on the interfacial normal stiffness which is difficult to measure accurately. Thus, we have chosen to treat ϵ_{eff}/ϵ as a free fitting parameter with an initial trial value 0.4.

Figure 7 shows the best fit obtained for $\Delta\bar{\mu}(\epsilon)$ at $V=1\ \mu\mathrm{m\,s^{-1}}$. It corresponds to $\epsilon_{eff}=0.48\epsilon$. From now on, all experimental data will be plotted versus this effective modulation parameter.

3. ac response

The computed first and second harmonics of the frictional response are plotted in Figs. 8(a) and 8(b). One can first note that the quasilinear dependence of μ_1 and μ_2 on V predicted by the perturbation calculation also holds here. Moreover, both computed harmonics saturate at large ϵ. None of these features agrees with the experimental behavior. We therefore conclude that, in spite of the excellent agreement between the predicted and observed $\Delta\bar{\mu}(\epsilon,V)$, the unmodified RR model is insufficient to describe the full response of the interface.

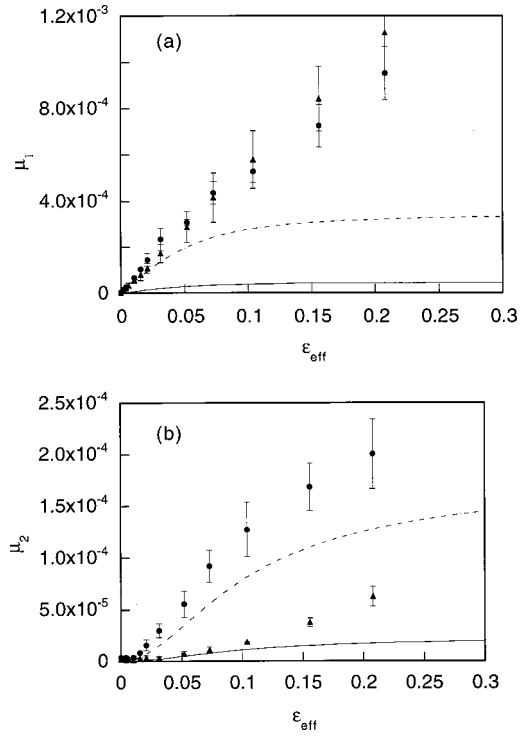

FIG. 8. Comparison between experimental data (symbols) and the RR model predictions (lines) at $f=120$ Hz for (a) $\mu_1(\epsilon_{eff})$ and (b) $\mu_2(\epsilon_{eff})$, at $V=1\ \mu\mathrm{m\,s^{-1}}$ (full line and triangles), and $V=10\ \mu\mathrm{m\,s^{-1}}$ (dashed line and circles).

B. Linker and Dieterich's aging law

As mentioned in Sec. I, Linker and Dieterich [2] (LD) proposed an extended version of the RR model in which the evolution law of the age variable Φ is modified according to Eq. (6). We now study the predictions of this extended model.

A perturbation calculation to first order in ϵ, using the equation of motion (8) and the age law (6), leads to a first harmonic amplitude

$$\mu_1 = \frac{\epsilon|\bar{\mu}-\alpha|}{A}\frac{V}{\omega}\frac{K}{W_0}. \tag{25}$$

This expression points to the fact that the dimensionless LD parameter α acts as a correction to the bare dynamic friction coefficient $\bar{\mu}$. For granite LD proposed $\alpha = 0.2$–0.3, i.e., a sizable fraction of $\bar{\mu}$ (≈ 0.6 for that material). This leads one to expect that such a value should induce significant effects on the predicted shear response. However, we have estimated [15] an order of magnitude of α for a sparse population of microcontacts (Greenwood interface [11]) aging under normal load. We have considered the two limits of (i) linear viscoelastic and (ii) fully developed plastic creep, using parameters compatible with the measured value of the RR parameter B. Both limits lead to the same estimate for α, namely, one order of magnitude smaller than the LD value. In view of this discrepancy, we have chosen to perform numerical integrations of Eqs. (8) and (6) for various values of α in the range 0.02–0.2.

The magnitude of the load modulation effect on $\Delta\bar{\mu}(\epsilon)$ depends strongly on α, as shown on Fig. 9(a). Whatever the value of α, $\Delta\bar{\mu}(\epsilon)$ remains quasi-independent of V, but for $\alpha = 0.2$ it is significantly smaller than the experimental one.

Moreover, the dependences of μ_1 and μ_2 on ϵ and V, shown in Figs. 9(b) and 9(c), as for the RR model, clearly disagree with the experimental results.

$\alpha = 0.02$ is found to provide a satisfactory fit for $\Delta\bar{\mu}(\epsilon)$. However, this α value is small enough for age effects to become negligible, as noted in Sec. III A 1. We indeed check [Figs. 9(b) and 9(c)] that the corresponding μ_1 and μ_2 are very close to those obtained from the unmodified RR model. We are thus led to conclude the following.

(i) The LD evolution law with their proposed value of α does not agree with the experimental results.

(ii) The $\Delta\bar{\mu}$ data permit one to set an upper limit on α without, however, allowing to check the validity of the functional form of the LD model. Experiments at much lower frequencies (comparable to the stick-slip frequency ω_c) would be needed to answer this question.

C. Extension of the RR model

The above analysis suggests that in our ''high frequency'' regime, where the response is controlled by the velocity modulations, it is the ''rheological'' factor $\sigma_s(\dot{x})$ which should be modified. As mentioned in Sec. I, σ_s describes the plastic dissipation occurring in a junction of nanometer thickness between contacting asperities, and the rate involved in σ_s is a rate of *irreversible* strain of this junction.

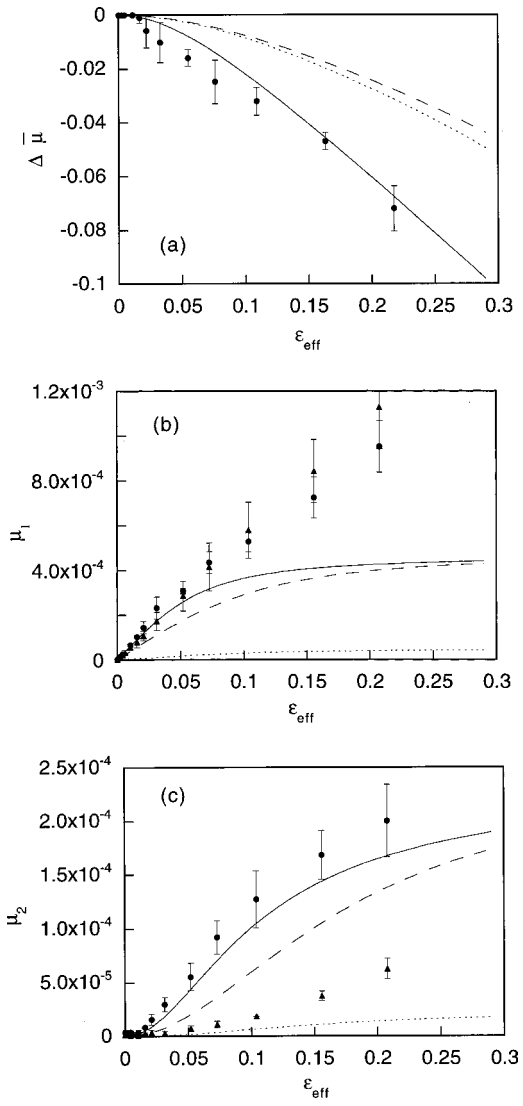

FIG. 9. Comparison between experimental data at $f = 120$ Hz and the LD model predictions for (a) $\Delta\bar{\mu}(\epsilon_{eff})$, (b) $\mu_1(\epsilon_{eff})$, and (c) $\mu_2(\epsilon_{eff})$. Lines: LD model for $V = 1\ \mu\mathrm{m\,s^{-1}}$ and $\alpha = 0.2$ (dotted line); $V = 10\ \mu\mathrm{m\,s^{-1}}$ and $\alpha = 0.2$ (dashed line), and $V = 10\ \mu\mathrm{m\,s^{-1}}$, $\alpha = 0.02$ (full line). The predictions for $V = 1\ \mu\mathrm{m\,s^{-1}}$ and $\alpha = 0.02$ are not plotted here because they would be undistinguishable from the dotted lines. Symbols: experimental data at $V = 1\ \mu\mathrm{m\,s^{-1}}$ (triangles) and $V = 10\ \mu\mathrm{m\,s^{-1}}$ (circles).

It has been shown [13] that when a multicontact interface is submitted to a shear much smaller than the static threshold, its response is elastic. Since the asperity ''bodies'' (which deform on a micrometric thickness, of the order of their diameter) are much more compliant than the nanometer-thick elastically pinned adhesive joint [10], it is their response which controls the interfacial shear stiffness κ_{asp}. This obeys an extended Amontons law, $\kappa_{asp} = W/\lambda$, with λ a length of order 1 μm for our surfaces.

Sliding amounts to a depinning of the adhesive joint which becomes dissipative, while the bodies of the asperities retain their elasticity. Therefore, we can schematically represent the sliding interface as an elastic element of stiffness κ_{asp}, accounting for the bulk elastic strain of the asperities, coupled in series to a (frictional) dissipative element (see

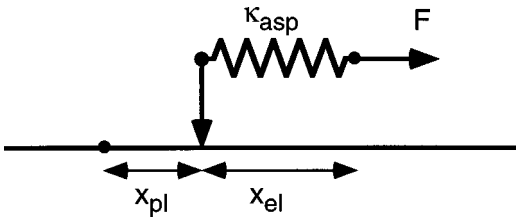

FIG. 10. Schematic rheological representation of the frictional interface (see text).

Fig. 10). When this latter is sheared at velocity $\dot{x}_{pl}$, the corresponding force is $F=f(\dot{x}_{pl})$,

$$F=\kappa_{asp}x_{el}=f(\dot{x}_{pl}), \tag{26}$$

with x_{el} and x_{pl} the elastic and irreversible displacements, respectively. The instantaneous velocity of the center of mass of the slider thus reads

$$\dot{x}=\dot{x}_{el}+\dot{x}_{pl}=\frac{d(F/\kappa_{asp})}{dt}+f^{-1}(F). \tag{27}$$

and the tangential force on the slider finally reads:

$$F=f\left(\frac{d}{dt}(x-F/\kappa_{asp})\right) \tag{28}$$

We therefore express the external force using the same functional form as in Eq. (1), but the argument of the rate-dependent term becomes $\dot{x}_{pl}$. In stationary sliding under constant normal load, F/κ_{asp} is constant; hence the usual dependence on $\dot{x}$. In the presence of a load modulation, both F and $\kappa_{asp}=W_0(1+\epsilon\cos(\omega t))/\lambda$ are modulated, and the elastic strain term becomes significant.

Hereafter we present results obtained from numerical integration of the corresponding extended RR equations. Taking into account the above-mentioned fact that in our experimental conditions, inertia can be neglected, Eq. (1) becomes

$$F/W=\frac{K}{W}(Vt-x)=\mu_0+A\ln\left[\frac{1}{V_0}\frac{d}{dt}\left(x-\frac{K}{\kappa_{asp}}(Vt-x)\right)\right]+B\ln\left(\frac{V_0\Phi}{D_0}\right). \tag{29}$$

The parameters A, B, and D_0 are set to their experimentally determined values. The length λ has been obtained from a quasi-static loading-unloading test [13] at various normal loads. We find $\lambda=0.62\pm0.15$ μm. In view of the relatively large experimental uncertainty on this parameter, we have integrated Eqs. (29) and (2), with λ as a free parameter. The best fit, performed on the most sensitive data, namely, the $\mu_1(\epsilon_{eff})$ ones, is found to correspond to $\lambda=0.7$ μm, within the experimental uncertainty bracket.

While $\Delta\overline{\mu}(\epsilon)$ is found to be only very weakly affected by the rheological correction, this extension of the model yields predictions for μ_1 and μ_2 markedly different from those of both the unmodified RR and LD models. That is, their quasilinear V-dependences are replaced by much weaker ones. On the other hand, neither μ_1 nor μ_2 exhibit any longer saturation within the relevant range $\epsilon_{eff}<0.3$. As appears from Fig. 11, the global agreement is now excellent, confirming the validity of the extended RR model.

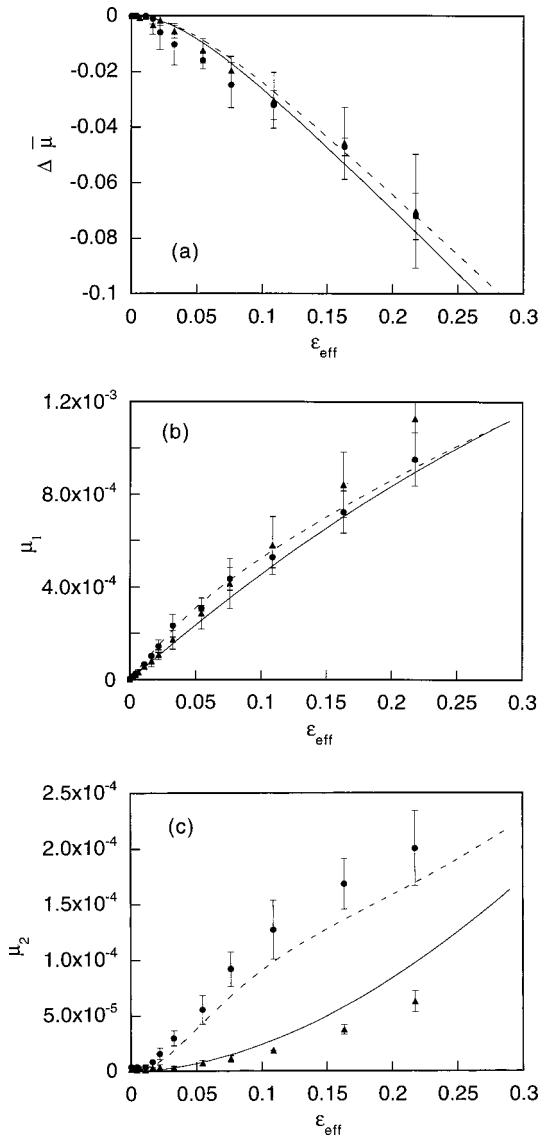

FIG. 11. Comparison between experimental data at $f=120$ Hz (symbols) and the *extended* RR model predictions (lines) for (a) $\Delta\overline{\mu}(\epsilon_{eff})$, (b) $\mu_1(\epsilon_{eff})$, and (c) $\mu_2(\epsilon_{eff})$ at $V=1$ μm s^{-1} (full lines and triangles) and $V=10$ μm s^{-1} (dashed lines and circles).

D. Concluding remarks

This study leads us to the following conclusions.

On the one hand, from an engineering point of view, the most spectacular effect of modulating the normal load applied to a frictional system is to lower the dynamic friction coefficient significantly. This occurs as soon as the modulation is applied, even though its amplitude is low enough to ensure permanent interfacial contact between the sliding bodies.

On the other hand, an important aim of this study was to elucidate the question, relevant to seismology, of whether the RR model should be modified to describe the frictional response to fast variations of the normal stress. We have shown that, in order to study this, it is essential to measure

and analyze not only the zero frequency component of the response to an oscillatory load, but also its harmonic content.

In the range of frequencies, much larger than the stick-slip one, that we have studied, the shear response is controlled by the velocity modulation, that is by the *rate-dependent* term of the RR constitutive law. However, the quantitative analysis of μ_1 and μ_2 data shows that the relevant displacement rate *is not*, for fast load modulations, *the slider velocity*, but the rate of plastic deformation of the adhesive frictional joint. This confirms our picture [10] of sliding friction as 2D plasticity prelocalized within a nanometer-thick adhesive joint coupled to the bulk of the slider through elastic asperities, and enables us to extend correspondingly the expression of the rate-dependent part of the RR state- and rate-dependent model.

The question of the precise nature of the effect of a load modulation on interfacial age remains at this stage open. That is, how should this effect be modeled? The only conclusion we can draw about this is that, at least for our system, if the Linker-Dieterich phenomenology is valid, then the magnitude they suggest for the modulation effect is strongly overestimated. Clearly, it is at frequencies of the order of the stick-slip one ω_c that the shear response is most sensitive to the age dynamics. This indicates that further investigations of this question should be performed in either of two ways: (i) working at modulation frequencies $\omega \simeq \omega_c$, or (ii) studying the low frequency content of the shear response to a high frequency modulation when crossing the stick-slip bifurcation line. Such work is presently in progress.

APPENDIX: ELASTOHYDRODYNAMIC RESPONSE OF THE INTERFACIAL AIR LAYER

The aim of this appendix is to establish the equation for the vertical motion of the slider (i.e., along the z direction normal to the interface) and to estimate the relative contributions of the forces that are involved. We will, as a result, justify the use of an *effective* amplitude of modulation of the normal load, to account for the fraction of the modulation which is borne by the air cushion trapped within the interfacial gap. The order of magnitude of this fraction, referred to as ϵ_{eff}/ϵ in the text, and which is the only fitting parameter of our model, is checked independently in a control experiment, performed *in vacuo*, and described in the text.

The motion of the slider along the z axis is assumed to be decoupled from the sliding motion along x. It is parametrized by the width h of the ''gap,'' i.e., the separation between the average planes passing through the rough surfaces of the track and the slider, respectively. When no modulation is superimposed on the bare normal load W_0, the width is h_0, a value fixed by the deformation of the load bearing asperities which are randomly distributed over the interface of nominal macroscopic area Σ_0.

(a) Elastic response of the multicontact interface. According to Greenwood and Williamson's model for multicontact interfaces, the number of load bearing asperities and the real area of contact increase linearly with the load. This induces a nonlinear dependence on load of the gap thickness. Experimentally, it has been found that $h_0 - h \simeq \lambda_z \ln(W/W_0)$, with λ_z a length, the order of magnitude of which is given by the roughness of the surfaces in contact (the standard deviation of the surface heights, here 1.3 μm). In the small amplitude linear regime ($\Delta h \ll \lambda_z$), the stiffness $\kappa_z = W/\lambda_z$ is a constant, and the elastic restoring force in the z direction reads

$$F_{el} \simeq W_0 \frac{(h-h_0)}{\lambda_z}. \tag{A1}$$

This expression has its exact counterpart for tangential motion, as discussed in the text. Shear elasticity involves a length λ which is expected ([17]) to be about $1.7\lambda_z$ for a Poisson ratio $\nu = 0.44$. Therefore, the measured value $\lambda = 0.7$ μm yields $\lambda_z \simeq 0.4$ μm.

(b) Elastohydrodynamic response of the interfacial air layer. When the gap is, e.g., narrowed, air is compressed until being drained out of the interfacial zone. The resulting pressure force on the slider will be denoted F_p. For the sake of evaluating F_p, we will simplify the problem, and consider a thin layer of air, of viscosity η and density ρ_0 at atmospheric pressure P_0, trapped between two *perfectly smooth* disks of radius R, parallel and distant of $h \ll R$. The relative velocity is supposed to vanish at $z=0$ and $z=h$, an assumption which is legitimate if the roughness of the surfaces is much smaller than the gap width. Brown and Scholz ([16]) reported measurement of the gap width between macroscopic ground glass surfaces. At a low average pressure corresponding to 10^{-5} of the Young modulus of the glass, as encountered in our experiments, they found that the gap width is typically five times larger than the rms roughness of the statistically identical surfaces. This figure is clearly too small for the ''smoothed'' model of the interfacial gap to be expected to provide a very accurate value of the hydrodynamic force, though it is certainly sufficient to estimate its order of magnitude.

An upper bound for the average pressure excess resulting from the motion of the disk is $\Delta P = \epsilon W_0/\Sigma_0$, with ϵW_0 the amplitude of the normal load modulation and $\Sigma_0 = \pi R^2$. The macroscopic loading pressure W_0/Σ_0 remains of order 10 mbar in the reported experiments, while ϵ is smaller than unity. As a result, ΔP remains much smaller than the atmospheric pressure P_0. However, the *compressibility* of the air layer may be of paramount importance, as suggested by the following argument. For infinite plates, no leak occurs at the edge of the gap and the response of the layer, trapped under the mean pressure P_0, is elastic with an overall stiffness:

$$\kappa_{air} = P_0 \Sigma_0 / h_0. \tag{A2}$$

For $P_0 = 10^5$ Pa, $\Sigma_0 = 49$ cm^2, and $h_0 = 6.5$ μm, one finds $\kappa_{air} = 7.5$ 10^7 N/m, namely, one order of magnitude larger than the interfacial stiffness κ_z originating from the load bearing asperities [see Eq. (A1)] at $W_0 = 7$ N. For a finite radius R, edge flow will reduce the amount of air to be compressed in order to accommodate the change of gap volume. It is therefore necessary to compute the expression of F_p by taking account the radial, viscosity controlled, Poiseuille flow which results from the density (hence pressure) gradient compatible with mass conservation.

The continuity equation for the radial flow reads

$$\frac{\partial}{\partial t}(\rho h) + \frac{1}{r}\frac{\partial}{\partial r}(r \overline{v} \rho h) = 0, \tag{A3}$$

where $\overline{v}(r)$ is the mean velocity at radius r (averaged across the gap along the z direction). The pressure field is given by the equation of state of the air at pressures close to $P_0=1$ atm, which is assumed to be

$$\frac{P}{\rho}=\frac{P_0}{\rho_0}. \tag{A4}$$

The set of equations is closed by assuming that the flow is of the Poiseuille type, namely, is parabolic along the z direction and varies slowly along the radial direction according to

$$\overline{v}=-\frac{h^2}{12\eta}\frac{\partial P}{\partial r}. \tag{A5}$$

As mentioned, the pressure modulation remains much smaller than P_0, and the gap modulation is smaller than h_0; hence linearization of Eqs. (A3)–(A5) is legitimate. One therefore sets $P=P_0+\delta P$, $\rho=\rho_0+\delta\rho$, and $h=h_0+\delta h$, with $\delta P \ll P_0$, $\delta\rho\ll\rho_0$ and $\delta h\ll h_0$. Eliminating $\delta\rho$ yields the following equation for the pressure field:

$$\frac{h^2}{12\eta}\frac{1}{r}\frac{\partial}{\partial r}\left(r\frac{\partial(\delta P)}{\partial r}\right)-\frac{\dot{\delta P}}{P_0}=\frac{\dot{\delta h}}{h_0}, \tag{A6}$$

where the dot indicates the partial derivative with respect to time.

Assuming that the normal elastic stiffness κ_z of the asperities remains linear, the gap modulation resulting from the normal load one is harmonic and we therefore seek for a complex solution to Eq. (A6) of the form $\delta P=\widetilde{\delta P}\exp(i\omega t)$, with $\delta h=\widetilde{\delta h}\exp(i\omega t)$. Taking into account the boundary condition $\delta P=0$ at $r=R$, and the symmetry requirement $\overline{v}=0$, and hence $\partial P/\partial r=0$, at $r=0$, one obtains

$$\widetilde{\delta P}=-P_0\frac{\widetilde{\delta h}}{h_0}\left[1-\frac{J_0(\gamma r)}{J_0(\gamma R)}\right], \tag{A7}$$

with J_0 the Bessel function of zeroth order, and γ a complex constant given by

$$\gamma=\frac{1-i}{\sqrt{2}}\sqrt{\frac{12\eta\omega}{P_0h_0^2}}. \tag{A8}$$

Integration of the pressure field over the interface yields the complex amplitude of the pressure force,

$$\widetilde{\delta F}_p=P_0\pi R^2\frac{\widetilde{\delta h}}{h_0}\frac{J_2(\gamma R)}{J_0(\gamma R)}. \tag{A9}$$

with J_2 the Bessel function of second order.

The asymptotic limits deserve comment. For $\gamma R\to\infty$ and $J_2/J_0\to-1$, $\widetilde{\delta F}_p$ is real, and one recovers the purely elastic response [Eq. (A2)] predicted for large R. It also corresponds to the high frequency limit for which the air has no time to leak. For $\gamma R\to 0$, $J_2/J_0\to(\gamma R)^2/8=-i\omega(3\eta R^2)/(2P_0h_0^2)$; hence $\widetilde{\delta F}_p$ is purely imaginary, and reduces to a linear viscous damping force which could have been derived by assuming a noncompressive Poiseuille flow. For intermediate values of γR, $\widetilde{\delta F}_p$ has both a reactive component, which increases the interfacial stiffness, and a dissipative component.

(c) Prediction for the effective amplitude of load modulation. The slider of mass M oscillates in the normal z direction under the combined action of the load modulation, the restoring elastic force resulting from deformation of the load bearing asperities and compression of the air cushion, and the damping force resulting from the air flow. The complex amplitude of modulation of the gap width $\widetilde{\delta h}$ is therefore given by

$$(-M\omega^2+\kappa_z)\widetilde{\delta h}-\widetilde{\delta F}_p=\epsilon W_0, \tag{A10}$$

with $\widetilde{\delta F}_p$ given by Eq. (A9).

The fraction of the load which is effectively borne by the microcontacts is $\epsilon_{eff}/\epsilon=|\kappa_z\widetilde{\delta h}/(\epsilon W_0)|$. It reads

$$\frac{\epsilon_{eff}}{\epsilon}=\left|1-\frac{\omega^2}{\omega_0^2}-\frac{\pi R^2P_0}{W_0}\frac{\lambda_z}{h_0}\frac{J_2(\gamma R)}{J_0(\gamma R)}\right|^{-1}, \tag{A11}$$

with $\omega_0=\sqrt{\kappa_z/M}$.

The assumption that ϵ_{eff}/ϵ does not depend on the amplitude of the modulation relies upon the fact that both the elasticity and viscosity remain linear; that is, as previously discussed, that $\Delta h\ll\lambda_z$ and h_0. This reduces to $\epsilon_{eff}\ll 1$, a criterion which is always fulfilled in our experiments.

For $W_0=7$ N, $M=1.6$ kg, $\lambda_z\simeq 0.4$ μm, and $\omega_0/(2\pi)=530$ Hz. Hence, at 120 Hz, the inertia is 5.2×10^{-2} of the elastic restoring force due solely to the asperities. It is clear from the above analysis that a key parameter for evaluating the viscoelastic response of the air is the gap width h_0. Taking, as discussed previously, the conservative value of five times the roughness, namely, $h_0=6.5$ μm, $\eta=10^{-5}$ Pa s, and $R=3.9$ cm, one computes $\gamma R=4(1-i)$ and $|\epsilon_{eff}/\epsilon|\simeq 0.24$, a value of the same order of magnitude than the one, namely, 0.48, which is found to provide the best agreement between the experimental data and the model prediction for $\Delta\overline{\mu}$. The role of the interfacial air cushion is further confirmed by the control experiment performed *in vacuo*. At a remaining pressure of 1 mbar, the elastic stiffness of the air layer falls two orders of magnitude below the multicontact one. Moreover, since the mean free path (at 300 K) of the gas molecules is now of order several 10 μm, i.e., larger than the gap width, the viscosity of the layer should vanish. Consequently, the effective amplitude is essentially ruled by the slider inertia according to $\epsilon_{eff}^{vacuum}/\epsilon\simeq|1-\omega^2/\omega_0^2|^{-1}=1.2$ at 200 Hz. At atmospheric pressure, keeping the nominal value $\Sigma_0=49$ cm^2, $\epsilon_{eff}^{air}/\epsilon=0.23$ at 200 Hz. When bringing the data for $\Delta\overline{\mu}(\epsilon)$ performed in the air and *in vacuo* to collapse on a single curve, as explained in the text, one makes use of a scaling ratio: $\epsilon_{eff}^{air}/\epsilon_{eff}^{vacuum}$. Its predicted value is 0.20. The experimental value is 0.4.

The fact that, in both cases, the estimated value is smaller than the observed one by the same amount may be possibly attributed to some long wavelength modulations of the gap width h_0 which is likely to remain after the lapping process. Microcontacts may be distributed on patches of macroscopic

area smaller than Σ_0, separated by regions of much wider gap in which the air would play a negligible role. Typically, a patch radius of 2.5 cm, while keeping the other parameters unchanged, would account for the observed value $\epsilon_{eff}/\epsilon \simeq 0.48$ at 120 Hz in the air. This would correspond to an effective area of $0.4\Sigma_0$, a value still large enough for the microcontacts—the number of which does not depend on Σ_0, according to Greenwood—to remain elastically independent. In addition, we have assumed a single degree of freedom for the slider, which is certainly a strong requirement since the slider is left free to find its own seat on the track. It is clear that a small amount of ''rocking'' would promote the air flow and reduce the cushion effect.

Finally, normal load modulation induces a tangential oscillating motion of the slider of amplitude Δx, and hence an air shear flow within the gap. The associated ac viscous force on the slider $\eta\omega\Delta x\Sigma_0/h_0$, which has been neglected in our models, must be compared to the leading term in the rate dependent friction force for oscillations about the sliding velocity V, namely, $AW_0\omega\Delta x/V$. The ratio of both terms is $\eta\Sigma_0 V/(W_0 h_0) \simeq 10^{-7}$ for $V=100$ μm/s; therefore, the shear viscosity of the layer is totally negligible.

[1] T. Skåre and J.-E. Ståhl, Wear **154**, 177 (1992).
[2] M. Linker and J. H. Dieterich, J. Geophys. Res. **97**, 4923 (1992).
[3] E. Richardson and C. Marone, J. Geophys. Res. **104**, 28 859 (1999).
[4] A. Cochard and J. Rice (unpublished).
[5] K. Ranjith and J. R. Rice, J. Mech. Phys. Solids (to be published)
[6] V. Prakash, J. Tribol. **120**, 97 (1998).
[7] J. R. Rice and A. L. Ruina, J. Appl. Mech. **105**, 343 (1983).
[8] F. Heslot, T. Baumberger, B. Perrin, B. Caroli, and C. Caroli, Phys. Rev. E **49**, 4973 (1994).
[9] F. P. Bowden and D. Tabor, *The Friction and Lubrication of Solids* (Clarendon, Oxford, 1950).
[10] T. Baumberger, P. Berthoud, and C. Caroli, Phys. Rev. B **60**, 3928 (1999).
[11] J. A. Greenwood and J. B. P. Williamson, Proc. R. Soc. London, Ser. A **295**, 300 (1966).
[12] For a recent review, see C. Marone, Annu. Rev. Earth Planet Sci. **26**, 643 (1998), and references therein.
[13] P. Berthoud and T. Baumberger, Proc. R. Soc. London, Ser. A **454**, 1615 (1998).
[14] poly(methyl-metacrylate), a vitreous polymer at ambient temperature, purchased under the name of ''Paraglas'' from Para-Chemie, Austria.
[15] T. Baumberger and C. Caroli (unpublished).
[16] S. R. Brown and C. H. Scholz, J. Geophys. Res. B **7**, 5531 (1985).
[17] H. A. Sherif and S. S. Kossa, Wear **151**, 49 (1991).